FREQUENCY BANDWIDTH OF HALF-WAVE IMPEDANCE REPEATER

Marek DVORSKY[1], *Libor MICHALEK*[1], *Martin TOMIS*[1]

[1]Department of Telecommunications, Faculty of Electrical Engineering and Computer Science, VSB–Technical University Ostrava, 17. listopadu 15, 708 33 Ostrava–Poruba, Czech Republic

marek.dvorsky@vsb.cz, marek.dvorsky@vsb.cz, martin.tomis@vsb.cz

Abstract. *This article brings in the second part general information about half-wave impedance repeater. The third part describes the basic functional principles of the half-wave impedance repeater using Smith chart. The main attention is focused in part four on the derivation of repeater frequency bandwidth depending on characteristics and load impedance of unknown feeder line. Derived dependences are based on the elementary features of the feeder lines with specific length. The described functionality is proved in part 4.3 by measurement of transformed impedance using vector several unbalanced feeder lines and network analyzer VNWA3+.*

Keywords

Impedance matching, impedance repeater, RF feeder line, Smith chart.

1. Introduction

The common issue in the antenna engineering is a transfer of general Antenna Input Impedance (AII) to the transceiver input terminal (TRX). It is often impossible to design conventional impedance matching circuits such as resonant-type matching circuits (e.g. Pi, T and Gamma) placed directly at the antenna terminals (e.g. wire-dipole antenna). The specific use of Impedance Repeater (IR) is its use such as a transmission line to connect multi-antenna arrays. Using IR to connect each single antenna still AII unchanged. The main characteristic of IR is that it can transform the load impedance with the ratio 1:1 from IR entry to IR output without its changing. On the IR output is available exactly the same impedance as AII is.

Simply described IR principle and the transferring function are valid only on the working frequency, where the Radio Frequency Line (RFL) has the length equal to the exact electrical half-wavelength. Throughout this article is made an analysis of the IR function and derivation its frequency bandwidth, which significantly expands the possibilities of usage the IR outside the working frequency.

2. Analysis of IR Function

Construction of linear wire antennas and its multiple uses at higher harmonics frequencies is in antenna practice commonly used routine. Such as a specific group of antennas is a dipole antenna, whose base resonant frequency is determined by its geometrical dimensions (length). A typical feature of the symmetric (center) feeds dipole is the high AII on the input terminal, where a symmetrical RFL is connected. The common issue needed to be solved at the IR end is to connect transformed AII to unbalanced RFL (usually coaxial RF cable with Characteristic Impedance (CI) $Z_0 = 50\ \Omega$).

Analysis of IR function can be derived from the basic function of tuned series quarter-wave RFL in the function of an impedance transformer [1]. Moreover, there are important limiting technical features of tuned series quarter-wave RFL described in [1], [2], [3]. Those mainly are RFL frequency bandwidth and losses expressed as attenuation of RFL. These losses include emission line losses in proportion to the value of CI Z_0 as well as losses in the tuned lines with standing waves (up to fivefold [4]), and so-called "*jump attenuation*" that appeared while greater rate impedances is connected at the end of the series quarter-wave RFL. Finally, also the skin effect as a result of pure high-resistance of RFL is necessary to take into account.

In all described examples and modifications of the RFL. It is automatically meant a balanced two-wire feeder. The same rules are also valid for the unbalanced feeders. Crucial for further analysis of IRL is Z_0 CI. It should be noted that this parameter is independent of the RFL length and used working frequency.

While designing the IRL, it is necessary to respect differences in electromagnetic waves velocity in the

air/vacuum and inside RFL. Electromagnetic energy propagation velocity depends on the relative permittivity ε_r describing dielectric environment between the feeder lines (1). In practice, the result of this difference is a different wavelength in a vacuum environment and in RFL environment [5], [6]:

$$\lambda = \frac{c}{f\sqrt{\varepsilon_r}}, \tag{1}$$

where c is the speed of electromagnetic waves in vacuum, f is the working frequency and ε_r is the relative dielectric constant of wave environment.

If $\varepsilon_r > 1$ than the wavelength is shrank relating to ε_r RFL material (compared to vacuum where $\varepsilon_r = 1$). Knowing the material constant ε_r of the IR, we are able to accurately determine real required geometrical IR length $\lambda/2$.

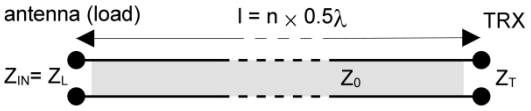

Fig. 1: Scheme of half-wave IR.

Changing the transformed impedance depending on RFL length can be expressed using the common formula (2), [1], [2], [5]:

$$Z(l) = Z_0 \frac{Z_L + jZ_0 \tan(\beta l)}{Z_0 + jZ_L \tan(\beta l)}, \tag{2}$$

where l is RFL length $l \in n\langle 0 \div 1\rangle \lambda$ (while IR l = 0,5 λ), Z_L is load impedance corresponding to AII, Z_T is a load impedance transformed to the end of RFL, Z_0 is RFL CI, β je wave number ($\beta = 2\pi/\lambda$).

The waveforms of real and imaginary impedance components $Z(l)$ is shown on Fig. 2. The point, where the imaginary impedance component passes through the zero, detects half-wave resonance (λ = 0,5 l). The value of the real part at this point has the equal value of $Z_T = Z_L$.

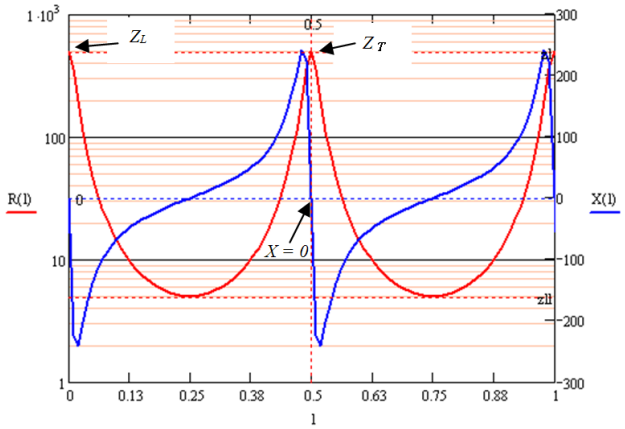

Fig. 2: The graph of the changing real (red) and imaginary (blue) components of transformed impedance depending on changing the length of the RFL, loaded impedance $Z_T = Z_L = 500 + 0j\ \Omega$.

3. Analysis of the IR in the Smith Chart

All consequences which occur in the transformation input (load) impedance Z_L to the output impedance Z_T will be displayed in the Smith Chart (SC). Convenience of using SC is that it allows monitoring all collectively important features in the context of one common diagram. SC transforms variables from a linear to bilinear space. This diagram clearly shows comprehensive energy functions and impedance changes in the investigate RFLs.

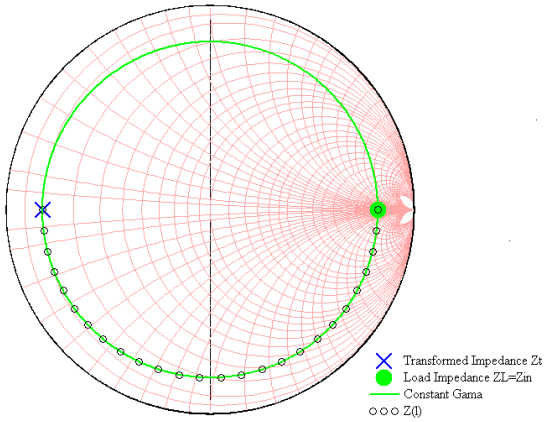

Fig. 3: Input impedance changes during the changing RFL length (l = 0 to 0,25 λ) in the SC.

Black circles in Fig. 3 shows the modification of the transferred load impedance at the output of the RFL while Z_T changing its length. The end of the RFL at a distance l = 0,25 λ (the source point - place at TRX) indicates a blue cross. Theoretically, the IR transforms a complex character impedance ($Z_L = R_L + jX_L$), [5]. In practical implementation, however, the function of IR working with complex load is distorted by primary lines parameters that supported on the Z_L. Thus affect the correct of IR function. Under given circumstances, purely real character load impedance ($Z_L \approx R_L$) is used for clear interpretation of the IR principles.

As an example, at the beginning of RFL (l = 0, blue dot Fig. 3) the RFL is loaded with a test load Z_L = 3 kΩ (the load ≈ AII Z_{IN}). The RFL CI is Z_0 = 300 Ω. The green circle on the Fig. 3 indicates the constant reflection coefficient Γ along the RFL. For RFL length l = 0,25 λ is the transformation of the input (load) impedance Z_L = 3 kΩ to the output impedance Z_T = 30 Ω, see (3), [1], [5]:

$$Z_T = Z_0 \frac{1+\Gamma}{1-\Gamma}, \tag{3}$$

$$\Gamma = \frac{Z_L - Z_0}{Z_L + Z_0}, \tag{4}$$

where Γ is the reflection coefficient (4), Z_T is the transformed impedance, Z_0 is the RFL CI. By adding a second section with length of 0,25 λ, it is obtained the total line length of 0,5 λ. The initial point (blue circle)

coincides with the end point (blue cross) shown in Fig. 4 (see the blue arrow). This is evidence that the impedance on the start and end of the RFL of the length $l = \lambda/2$ is the same, so $Z_L = Z_T$.

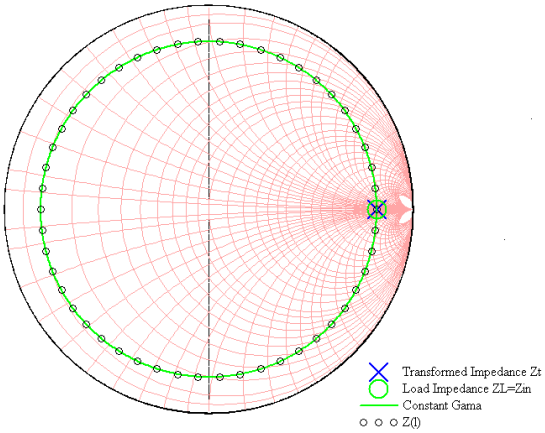

Fig. 4: The input impedance changes during the changing line length (l = 0 to 0,5 λ).

4. Derivation of the IR Bandwidth Depending on CI

As described in the previous chapter, the main prerequisite of using RFL as IR is that its exact length is $n \times 0{,}5\ \lambda$. The next step is to define the boundary conditions which determine the resonance frequency bandwidth of RLC circuits at which the RFL still working as IR. The following text describes the basic situation for the single half-wavelength RFL, i.e. $n = 1$.

4.1. Determination of IR Bandwidth

RFL can be considered as series RLC resonant circuit. The resonant point occurs in a situation where the imaginary component of impedance $Z(l)$ is zero, see Fig. 2, (resonant frequency f_0). The derivation of the frequency bandwidth of the impedance described by formula (2) is difficult to implement using basic formulas from the issue of RLC circuits. These are based on the knowledge of the circuit quality factor Q at resonance (5), [2]:

$$Q = \frac{X_{L0}}{R_0}, \tag{5}$$

where R_0 is the resistance loss of serial RLC circuit at the resonant frequency f_0 ($Z_0 \approx R_0$), X_{L0} is resonant reactance at f_0 ($|X_{C0}| = X_{L0}$). The resulting value of resonant reactance is $X_{L0} + X_{C0} = 0$. Through formula (2), it can be derived only summarizing final component $X = X_L + X_C$. From the known values of X, it cannot be re-derive the individual contributions X_L and X_C and thereby further define Q by formula (5). Reactive values of L and C cannot be measured using either type of antenna analyzers such as *MFJ269* [7] or *AA520* [8]. If there is a known RFL datasheet with the values of feeder capacity, than Q can be calculated according to (5) and the bandwidth can be derived according to the known relations (6) and (7), [9]:

$$B = \frac{f_0}{Q} = f_h - f_d, \tag{6}$$

$$f_{d,h} = \frac{\pm 1 + \sqrt{1 + 4Q^2}}{2Q}. \tag{7}$$

However, if there is an unknown RFL then the derivation of IR bandwidth should be undertaken in the manner described as follows. Generally, a valid condition for determining the working bandwidth at resonance (i.e. setting f_d as a lower and f_h as an upper frequency) is a 50 % decrease of real power component compared to the value of the resonance point. The 50 % energy decrease in the complex impedance circuit arises when the real and imaginary components of impedance are equal ($Z = a + j \cdot a$). This point can be easily identified in the phase chart where the phase achieves value $\pm \pi/4$ (Fig. 5), formula (8):

$$f_{d,h} \approx \arg\left(Z(l)\right) \pm n\frac{\pi}{4} = 0. \tag{8}$$

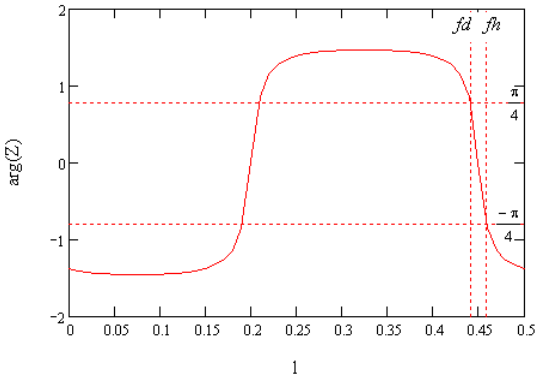

Fig. 5: The phase chart of impedance Z_T depending on the wavelength of the RFL.

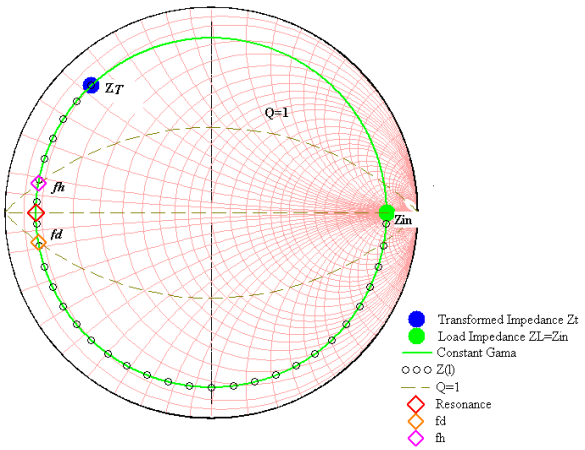

Fig. 6: IR bandwidth in the SC ($Q = 1$ brown dashed line corresponding to 50 % energy decrease, the resonance point - red, f_d - orange, f_h - pink rhomboid), $\Gamma \rightarrow 1$, $f_h - f_d = B \rightarrow 0$.

The roots of the equation (8), (i.e. the phase meets value $\pm \pi/4$) might find in close to half-wave resonance. The SC clearly shows the place where $R = X$ with a line of the quality factor $Q = 1$. Resonance is located on the real line diagram (Fig. 6).

4.2. Bandwidth Derivation Depending on CI Z_0

IR frequency bandwidth B is given by changing the transformed impedance different less than 50 % from the initial value (at resonance), which corresponds to a decrease of a real energy component by -3 dB. In the SC can be seen that the limit points f_d and f_h are always moving along the curve corresponding to $Q = 1$ ($R = X$) (Fig. 6 - black arrows). Subsequently, it can be derived that the bandwidth increases with decreasing radius of reflection coefficient Γ circle (green circle in Fig. 6). The closer to the edge of the diagram the working point is ($\Gamma \to 1 \approx \text{PSV} \to \infty$), more the IR selective $B \to 0$ is (see example in Fig. 6). The reverse extreme shows situation where the load impedance Z_L is near to the characteristic impedance Z_0. Then, the $\Gamma \to 0 \approx \text{PSV} \to 1$ (see example in Fig. 7, sub-index *"b"*), thus IR becomes a wild-broadband ($B \to B_{max}$), [3], [10].

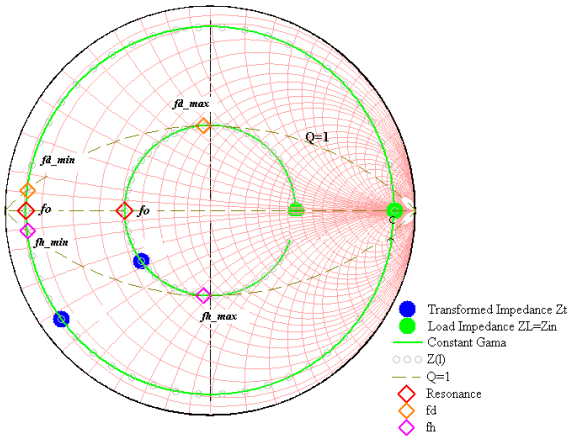

Fig. 7: IR bandwidth in the SC ($Q = 1$ brown dashed line corresponding to the resonance point - red, f_d - orange, f_h - pink rhomboid), $f_{h\_max} - f_{d\_max} = B \to B_{max}$.

The bandwidth itself is not only a function of CI Z_0, but also function of the value Z_L. In particular, B is the function of the ratio Z_0 and Z_L. It can be generalized that IR frequency bandwidth is dependent on the Standing Wave Ratio (*SWR*). Value B_{max} is reached when a decrease of the real part of impedance Z_L will not cause further decline below 50 % in real power at resonance point. This point occurs when the change of Z_{L0} (the value of load impedance at a working frequency) reaches such values that are currently $|Z_L| = Z_{L0}$ and at the same time $Q = 1$ (point f_h and f_d in Fig. 7).

Furthermore, the impedance value can be derived from the limit points f_d and f_h (9):

$$Z_{L_{dh}} = \frac{Z_{L0}}{\sqrt{2}}(1 \pm i). \tag{9}$$

These impedances limit corresponds to reflection Γ_{lh} and SWR_{lh} (10), (11):

$$\Gamma_{lh} = \left|\frac{\left(1-\sqrt{2}\right)+i}{\left(1+\sqrt{2}\right)+i}\right| = 0,414\,, \tag{10}$$

$$SWR_{lh} = \frac{1+|\Gamma_{lh}|}{1-|\Gamma_{lh}|} = 2,414\,. \tag{11}$$

For the typical balanced line with CI $Z_0 = 300\ \Omega$, there are the limiting values of $Z_L = 124{,}264\ \Omega$ and 724,264 Ω. Thus, if a load is connected to the IR $Z_L \in \langle 124{,}264 \div 724{,}264\rangle\ \Omega$, then changing the working frequency does not invoke the change transformed Z_T. IR output that never exceeds the value would cause a decline in the real part of the performance below 50 % power at resonance point. Theoretically, the ratio between the load impedance and Z_0 $SWR < 2{,}414$, the $B \to \infty$.

If the $SWR > 2{,}414$, then from the SC can be derived frequency bandwidth of IR as the distance equal f_d and f_h and set the following formula (12):

$$B(SWR) = b \cdot f = \frac{\arg|\Gamma|}{\pi} \cdot f = \frac{\arg\left(\frac{SWR-1}{SWR+1}\right)}{\pi} \cdot f_0\,, \tag{12}$$

where b is an argument of Γ divided by π. Dependence IR bandwidth, which transforms the Z_L $SWR > 2{,}414$ has an exponential character (Fig. 8).

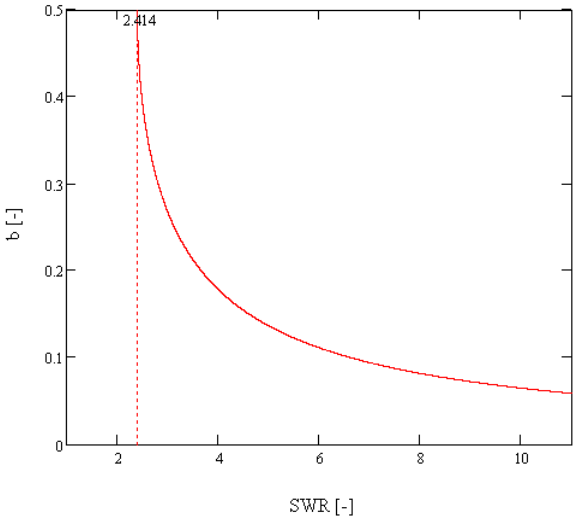

Fig. 8: Dependence of IR bandwidth to SWR ($B = b\ f_0$).

4.3. Validation of Derived Relations

Validation of the considerations that had led to the derivation of formulas (8) to (11) was performed on several samples of asymmetrical RF cable RG58 ($Z_0 = 50\ \Omega$). Unbalanced cable was used due to

unbalanced inputs of *MFJ269* [7], *AA250* [8] and *VNWA3+* analyzers [11]. Finding half-wave resonance frequency was calculated using velocity factor 0,66 according to the manufacturer's data sheet. The actual transformed load impedance was carried out by vector network analyzer *VNWA3+*. Measured frequency bandwidth $B(SWR)$, which was determined from the limits Z_T points (f_d and f_h) while changing the load impedance Z_L (i.e. changing *SWR*) corresponding to the derivative in values from formula (11). The primary line parameters were also taken into account, which was detected as a systematic measurement error.

5. Conclusion

This article describes the specific feature of RFL with length of $n \times 0{,}5\ \lambda$ so-called Half-Wave Impedance Repeater. The main objective of the article is to define the frequency bandwidth of IR in connection to its characteristic impedance. It has been proved that derived bandwidth is not only dependent on its own impedance Z_0, but is also influenced by the ratio between the load transferred impedance Z_L and characteristic impedance Z_0. This correlation is described by a standing waves ratio (3), (4). Graphic dependence of IR bandwidth is shown in Fig. 8. The derived function has an exponential character. As the limit value was detected, the *SWR* value of 2,414 from which the IR becomes wide-bandwidth.

Theoretically derived assumptions were verified by measuring on the unbalanced cable via RF vector network analyzer *VNWA3+*. These measurements confirmed described relations (8) to (11). Purely real variable loads Z_L were used during the measurements. However, the real part of AII is frequency dependent. This dependence does not change the validity of formula (11) since it does not depend only on the R_L, but generally on the *SWR*.

In further work, the research team wants to focus on the influence of frequency-variable primary IR parameters and their influence on IR bandwidth. It will also examine the influence of IR bandwidth on the nth length IR section.

Acknowledgements

The research leading to these results has received funding from the Grant SGS no. SP2012/180, “Changes in radio signal propagation due to weather condition”.

References

[1] REGIER, F.A. Impedance matching with a series transmission line section. *Proceedings of the IEEE*. 1971, vol. 59, iss. 7, pp. 1133-1134. ISSN 0018-9219. DOI: 10.1109/PROC.1971.8354.

[2] The American Radio Relay League, Inc. *The ARRL antenna Book*. 19th Edition. Newington: ARRL Amateur Radio, 2000. ISBN 0-87259-817-9.

[3] WELLER, Albert, E., Jr. Series Section Transmission Line Transformers. In: *National Radio Astronomy Observatory* [online]. 2010. Available at: http://www.tuc.nrao.edu/~demerson/weller/weller.pdf.

[4] IKRENYI, Imrich. *Amaterske kratkovlnne anteny*. Bratislava: Alfa, 1972.

[5] HUANG, Yi and Kevin BOYLE. *Antennas: from theory to practice*. Chichester: John Wiley & Sons, 2008. ISBN 978-0470510285.

[6] BALANIS, Constantine, A. *Antenna theory: analysis and design*. 3rd ed. Hoboken: John Wiley & Sons, 2005. ISBN 978-0471667827.

[7] MFJ-269: HF/VHF/UHF SWR ANALYZER. *MFJ* [online]. 2012. Available at: http://www.mfjenterprises.com.

[8] RigExpert AA-520: *Antenna Analyzer*. [online]. Available at: http://www.rigexpert.com/index?s=aa520.

[9] ZALUD, Vaclav. *Moderni radioelektronika*. 1st ed. Praha: BEN-Technicka literatura, 2000. ISBN 80-860-5647-3.

[10] ALLEN, W.N., J. SMALL, L. XIAOGUANG and D. PEROULIS. Bandwidth-optimal single shunt-capacitor matching networks for parallel RC loads of Q>>1. In: *Microwave Conference, 2009. APMC 2009.: Asia Pacific*. Singapore: IEEE, 2009, 2128 - 2131. ISBN 978-1-4244-2802-1. DOI: 10.1109/APMC.2009.5385256.

[11] DG8SAQ VNWA 3+: Vector Network Analyzer. *SDR-Kits* [online]. 2012 [cit. 2012-10-29]. Available at: http://sdr-kits.net/.

About Authors

Marek DVORSKY was born in 1981. He received his Ph.D. from Department of Telecommunications, Faculty of Electrical Engineering and Computer Science, VSB–Technical University Ostrava in 2009. His research interests include new digital radio-communication technologies and antennas engineering.

Libor MICHALEK was born in 1979. He received his Ph.D. from Department of Telecommunications, Faculty of Electrical Engineering and Computer Science, VSB–Technical University Ostrava in 2008. His research interests include new digital telecommunication technologies.

Martin TOMIS was born in 1987. He received his master degree from Department of Telecommunications, Faculty of Electrical Engineering and Computer Science, VSB–Technical University Ostrava in 2011. His research interests include virtual instrumentation.